Delft University of Technology

Transparent silicon carbide/tunnel SiO_2 passivation for c-Si solar cell front side Enabling J_{sc} > 42 mA/cm^2 and iV_{oc} of 742 mV

Pomaska, Manuel; Köhler, Malte; Procel Moya, Paul; Zamchiy, Alexandr; Singh, Aryak; Kim, Do Yun; Isabella, Olindo; Zeman, Miro; Li, Shenghao; More Authors

Important note
To cite this publication, please use the final published version (if applicable).
Please check the document version above.

RESEARCH ARTICLE

PROGRESS IN PHOTOVOLTAICS WILEY

Transparent silicon carbide/tunnel SiO$_2$ passivation for c-Si solar cell front side: Enabling J_{sc} > 42 mA/cm^2 and iV$_{oc}$ of 742 mV

Manuel Pomaska[1] | Malte Köhler[1] | Paul Procel Moya[4] |
Alexandr Zamchiy[2,3] | Aryak Singh[1] | Do Yun Kim[1] | Olindo Isabella[4] |
Miro Zeman[4] | Shenghao Li[1,5] | Kaifu Qiu[1,5] | Alexander Eberst[1] |
Vladimir Smirnov[1] | Friedhelm Finger[1] | Uwe Rau[1] | Kaining Ding[1]

[1]IEK5-Photovoltaics, Forschungszentrum Jülich, Wilhelm-Johnen-Strasse, Jülich, 52425, Germany

[2]Novosibirsk State University, Physics Department, Pirogova St 2, Novosibirsk, 630090, Russia

[3]Kutateladze Institute of Thermophysics SB RAS, Laboratory of Rarefied Gases, Ac. Lavrentiev Ave 1, Novosibirsk, 630090, Russia

[4]PVMD Group, Delft University of Technology, Mekelweg 4, Delft, 2628, CD, The Netherlands

[5]Institute for Solar Energy Systems, Guangdong Provincial Key Laboratory of Photovoltaic Technology, Sun Yat-sen University, Guangzhou, 510006, China

Correspondence
Manuel Pomaska, IEK5-Photovoltaics, Forschungszentrum Jülich, Wilhelm-Johnen-Strasse, Jülich 52425, Germany.
Email: m.pomaska@fz-juelich.de

Abstract

N-type microcrystalline silicon carbide (μc-SiC:H(n)) is a wide bandgap material that is very promising for the use on the front side of crystalline silicon (c-Si) solar cells. It offers a high optical transparency and a suitable refractive index that reduces parasitic absorption and reflection losses, respectively. In this work, we investigate the potential of hot wire chemical vapor deposition (HWCVD)–grown μc-SiC:H(n) for c-Si solar cells with interdigitated back contacts (IBC). We demonstrate outstanding passivation quality of μc-SiC:H(n) on tunnel oxide (SiO$_2$)–passivated c-Si with an implied open-circuit voltage of 742 mV and a saturation current density of 3.6 fA/cm^2. This excellent passivation quality is achieved directly after the HWCVD deposition of μc-SiC:H(n) at 250°C heater temperature without any further treatments like recrystallization or hydrogenation. Additionally, we developed magnesium fluoride (MgF$_2$)/silicon nitride (SiN$_x$:H)/silicon carbide antireflection coatings that reduce optical losses on the front side to only 0.47 mA/cm^2 with MgF$_2$/SiN$_x$:H/μc-SiC:H(n) and 0.62 mA/cm^2 with MgF$_2$/μc-SiC:H(n). Finally, calculations with Sentaurus TCAD simulation using MgF$_2$/μc-SiC:H(n)/SiO$_2$/c-Si as front side layer stack in an IBC solar cell reveal a short-circuit current density of 42.2 mA/cm^2, an open-circuit voltage of 738 mV, a fill factor of 85.2% and a maximum power conversion efficiency of 26.6%.

KEYWORDS
antireflecting coating, excellent passivation, heterojunction, hot wire CVD, lean process, refractive index, silicon carbide, tunnel oxide

1 | INTRODUCTION

Crystalline silicon (c-Si) solar cells have reached energy conversion efficiencies above 26%,[1,2] with the help of full area selective passivating contacts. For such high conversion efficiencies, intrinsic amorphous silicon (a-Si:H(i)) and ultrathin tunnel oxide (SiO_2) have become the predominant materials for the passivation of c-Si surfaces.[3] A comparison of both passivation concepts shows that record cells with a-Si:H(i) passivation developed for the silicon heterojunction (SHJ) technology currently give rise to higher open-circuit voltages (V_{oc}) than using SiO_2 passivation[3] from polycrystalline silicon on oxide (POLO) technology or tunnel oxide passivating contact (TOPCon) technology. Further, for a-Si:H(i), the excellent interface passivation is directly achieved after the deposition of the a-Si:H(i) film, whereas for SiO_2, it requires several additional process steps to provide excellent interface passivation.[4] Reducing the number of process steps is under current investigation within several research groups in the field of c-Si solar cells. Although a-Si:H(i) is an excellent passivation material, it possesses an optical bandgap[5] of approximately 1.7 eV that leads to significant parasitic absorption of the incident sunlight.

N-type microcrystalline silicon carbide (μc-SiC:H(n)) grown by hot wire chemical vapor deposition (HWCVD) is known for its large optical bandgap[6–7] of 2.4 to 3.4 eV. This high optical transparency makes it a promising window layer material,[8] which was developed for silicon thin-film solar cells[9] as well as for silicon heterojunction solar cells,[7,10] However, the deposition conditions for growing highly transparent μc-SiC:H(n) on top of a-Si:H(i) lead to strong deterioration of the underlying amorphous silicon layers, because of etch-off of the films,[6,8,11] This trade-off between high-quality passivation and attractive transparency has limited the beneficial implementation of μc-SiC:H(n) in silicon solar cells for a long time. In the past, we showed that it is possible to fabricate symmetric test structures, where the layer stack of HWCVD-grown μc-SiC:H(n) on tunnel SiO_2 passivated the c-Si surfaces. We achieved high passivation quality with implied open-circuit voltages (iV_{oc}) of up to 728 mV and saturation current densities (J_0) down to 7.1 fA/cm² on double-side textured c-Si wafers,[7,12] We further reported on the corresponding contact resistivities derived in the cited references, where the lowest value[7] was 18 mΩcm². These promising results were achieved directly after the HWCVD deposition of μc-SiC:H(n) and without any further treatments, eg, annealing or hydrogenation. Because of the large optical bandgap of μc-SiC:H(n), we named the layer stack of μc-SiC:H(n)/SiO_2/c-Si *transparent passivating contact* (TPC) in the past.[7,12]

So far, the TPC was only used for two side contacted c-Si solar cells,[7,12] where it replaced the a-Si n-layer and i-layer of the front side by transparent μc-SiC:H(n)/SiO_2. Additionally, it is possible to contact the TPC with indium tin oxide and conventional low-temperature screen-printed silver contacts, in order to use it as a font side c-Si solar cell concept.

In this work, we investigate the potential of the transparent μc-SiC:H(n)/SiO_2 passivation layer stack used as part of an antireflection coating (ARC) for the front side of a c-Si solar cell with interdigitated
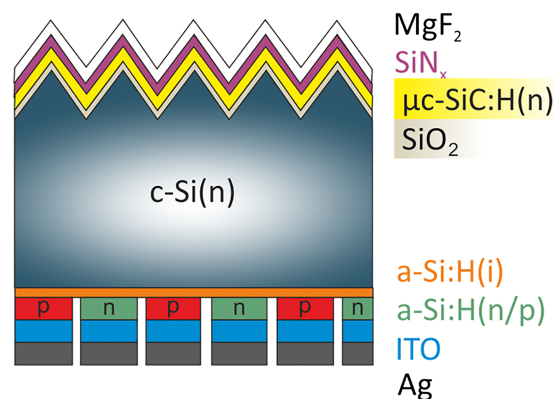

FIGURE 1 IBC c-Si solar cell with triple-layer ARC developed in this work. The triple-layer ARC consists of a 108 nm-thick MgF_2 layer, a 50- to 60 nm-thick SiN_x layer, and a 0- to 60 ?]nm-thick μc-SiC:H(n) layer. At the same time, the μc-SiC:H(n)/SiO_2 stack provides excellent surface passivation [Colour figure can be viewed at wileyonlinelibrary.com]

back contacts (IBC) as illustrated in Figure 1. The concept of IBC offers the possibility to achieve highest short-circuit current densities (J_{sc}), because of the absence of shading metal contacts on the front side. We developed an ARC consisting of magnesium fluoride (MgF_2), silicon nitride (SiN_x:H), and μc-SiC:H(n) as illustrated in Figure 1. For that purpose, it was important to tune the thickness of μc-SiC:H(n) for a minimum total optical loss of parasitic absorption and reflection.

The J_{sc} of the currently best silicon-based solar cells are 42.9 mA/cm²,[13] for Fraunhofer ISE *TOPCon*,[13] 42.7 mA/cm² for Kaneka *SHJ-IBC*,[1] 42.6 mA/cm² for ISFH *POLO-IBC*,[2] and 42.7 mA/cm² for UNSW *PERL*.[14] All J_{sc} values of the record cells are above 42 mA/cm², but they were either achieved by many process steps or undisclosed fabrication processes. Thus, the goal of this work was to develop a transparent passivation as part of an ARC for the front side of IBC c-Si solar cells using a lean process flow that gives rise to very high J_{sc} values above 42 mA/cm².

2 | EXPERIMENTAL DETAILS

The μc-SiC:H(n) layers were deposited in an HWCVD vacuum chamber with three curled rhenium wires, 6-sccm flow rate of the monomethylsilane (MMS) gas, which is diluted to 5% in H_2, 94-sccm flow rate of the H_2 gas, 75-Pa chamber pressure, 250°C heater temperature, and 1800°C filament temperature. SiN_x layers were deposited in a plasma-enhanced chemical vapor deposition chamber using 7.8 sccm of SiH_4 and 10 sccm of NH_3 diluted in 450 sccm of Argon and 138 sccm of Helium. The chamber pressure was 8 Pa, the heater temperature was 100°C, and the inductive coupled plasma power was 700 W. MgF_2 layers were thermally evaporated at room temperature. All films were deposited on glass substrates (Corning, EAGLE XG). We derived the complex refractive index for the 130 nm μc-SiC:H(n) film by fitting the reflectance and transmittance spectra with the SCOUT software.[15] The reflectance and transmittance

spectra were measured with a PerkinElmer Lambda 950 UV-Vis spectrophotometer.

Lifetime samples and ARC samples were processed onto double-side textured, phosphorus-doped, Czochralski grown, and <100> orientated c-Si wafers with a resistivity of 1.0 Ωcm and a thickness of 170 μm. The wafers were cleaned using complete RCA (Radio Corporation of America) treatment. After dipping in diluted hydrofluoric acid (HF) for 10 minutes to remove the oxide, the tunnel oxide was grown for 10 minutes on both sides of the wafer in a piranha solution (H_2O_2: H_2SO_4) at 60°C. Details of the wet-chemical preparation can be found elsewhere.[11] According to spectroscopic ellipsometer measurements of the tunnel oxide on flat <111> orientated wafer the SiO_2 thickness was approximately 1.2 nm. For lifetime samples, the μc-SiC:H(n) layers had a thickness of 30 nm. The thickness, the complex refractive index, and the extinction coefficient of SiN_x and MgF_2 were obtained by using the SENTECH SE-800 ellipsometer.

The reflectance spectra of the ARC samples were recorded using the LOANA measurement system from pv tools. To simulate optical losses for different ARC stack designs, we used OPAL2 software provided by PV Lighthouse[16] with the measured complex refractive indices of the thin films as input parameters. For the c-Si surface morphology, we assumed randomly distributed, upright pyramids with a characteristic angle of 54.75° as confirmed by SEM images, and a planar fraction of 8%. For the light trapping model, we assumed a substrate thickness of 170 μm. Lastly, potential short-circuit current densities were calculated by means of Monte Carlo ray tracing technique in combination with the transfer matrix method boundary conditions[17] within Sentaurus TCAD.[18] Models and parameters are detailed elsewhere.[19,20] To highlight the effect of proposed front ARC, we performed the numerical simulations using optimized layer stacks and rear side geometry as described in Procel et al[19] but adapted for 170-μm-thick c-Si wafer with a resistivity of 1 Ωcm.

3 | RESULTS

Before the development of an excellent ARC using HWCVD grown μc-SiC:H(n) for IBC-SHJ solar cells, symmetric test structures of μc-SiC:H(n)/SiO_2/c-Si(n)/SiO_2/μc-SiC:H(n) were fabricated to optimize the passivation of the c-Si surface. The thickness of the μc-SiC:H(n) films was in the range of 30 to 40 nm. The effective charge carrier lifetimes as a function of minority carrier density of two identically prepared samples with the best passivation quality are shown in Figure 2. The corresponding iV_{oc} values at 1 sun illumination are 742 mV for both samples. The values for J_0 are 3.6 and 3.7 fA/cm². Although, after HF-dipping of the test structures, the passivation quality in terms of iV_{oc} and J_0 is unchanged, the growth of an additional SiN_x:H or MgF_2 layer deteriorates the passivation quality significantly. However, it can be restored by annealing of the sample at 230°C for 20 minutes on a hot plate.

To develop the MgF_2/SiN_x:H/μc-SiC:H(n) ARCs, the refractive indices (n) and the extinction coefficients (k) were derived from ellipsometry and UV-Vis-spectroscopy, respectively, for μc-SiC:H(n),
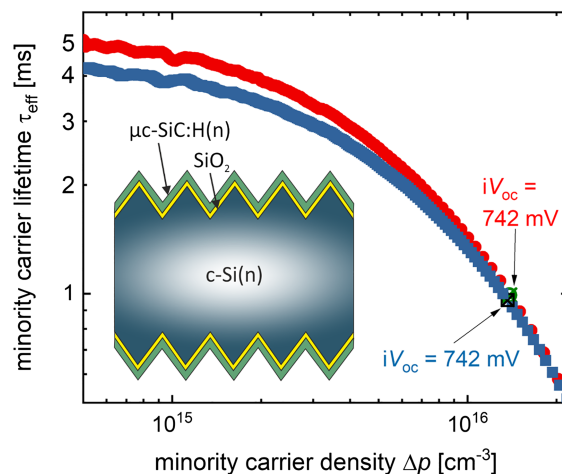

FIGURE 2 Effective carrier lifetime τ_{eff} as a function of minority carrier density Δ_p of two double-side textured wafers (phosphorus-doped, Czochralski, resistivity of 1.0 Ωcm, and thickness of 170 μm) passivated by SiO_2/μc-SiC:H(n). For both samples, the implied open-circuit voltage at 1 sun illumination is 742 mV measured directly after the HWCVD deposition of μc-SiC:H(n). No further postdeposition treatment was applied [Colour figure can be viewed at wileyonlinelibrary.com]
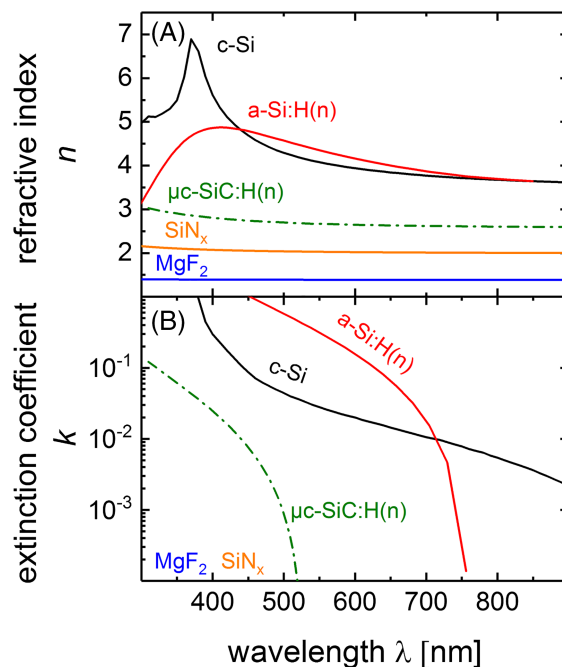

FIGURE 3 (A) Refractive index n and (B) extinction coefficient k derived from ellipsometry measurements of μc-SiC:H(n), SiN_x, MgF_2, a-Si:H(n),[5] and c-Si.[21] The derived k is zero for SiN_x and MgF2. The full sets of n and k data for μc-SiC:H(n), SiN_x, and MgF_2 can be found in the Supporting Information S1, S2 and S3 [Colour figure can be viewed at wileyonlinelibrary.com]

SiN_x:H, and MgF_2. The results are plotted in Figure 3 as a function of wavelength together with n and k of c-Si[19] and a-Si:H(n).[20] The refractive index of MgF_2 is 1.4, of SiN_x:H is 2.0 to 2.2, and of μc-SiC:H(n) is 2.6 to 3.0 over the wavelength range of 300 to 900 nm. Within the

same wavelength range n is 3.6 to 6.9 for c-Si and 3.1 to 4.9 for a-Si. The extinction coefficients derived for MgF_2 and of SiN_x:H are zero over the whole wavelength range. For μc-SiC:H(n), the edge of k ($k = 10^{-4}$) is at 520 nm, while it is at 750 to 760 nm for a-Si and at 1050 nm for c-Si. The full sets of n and k data for μc-SiC:H(n), SiN_x:H, and MgF_2 can be found in the Supporting Information.

Using the obtained refractive indices as input parameters for OPAL2 simulations, the spectral reflectance of the MgF_2/SiN_x:H/μc-SiC:H(n)/SiO_2/c-Si stack was calculated for different thicknesses of μc-SiC:H(n) (d_{SiC} = 0-60 nm). The thickness of MgF_2 was kept constant at 100 nm, and SiN_x:H thickness was varied between 50 and 60 nm. To be able to compare these results, we fabricated all the triple-layer stacks and measured the reflectance. The results of the simulated reflectance can be found in Figure 4A, while the results of the measured reflectance are shown in Figure 4B. In order to deposit the exact thickness of each layer, the individual thicknesses were adjusted from a reference sample beforehand, using the cross section pictured by scanning electron microscopy (Figure 4C) for thickness measurement of the layers. The resulting simulated and measured reflectance spectra are in very good agreement with each other.

To quantify the reflection losses, we multiplied the simulated and measured reflectance spectra of Figure 4 with the AM1.5 sun spectrum and integrated the result from 300- to 990 nm wavelength. The results are current density losses of J_{sc} due to reflection as a function of d_{SiC} (Figure 5). We observe that the simulated reflection current

FIGURE 5 Optical losses of current density on front side of IBC c-Si solar cell with triple-layer ARC (see Figure 1) as a function of the μc-SiC:H(n) layer thickness. Presented are (A) simulated and (B) measured current loss densities rising from parasitic absorption and reflection loss. Measured current loss densities were obtained from fabricated ARC samples. To calculate the current loss due to reflection, the reflectance spectra (Figure 4) were multiplied by the AM1.5G spectra and then integrated from 300 to 990 nm that were used for integration. Parasitic absorption loss was calculated from k data of μc-SiC:H(n) shown in Figure 3B [Colour figure can be viewed at wileyonlinelibrary.com]
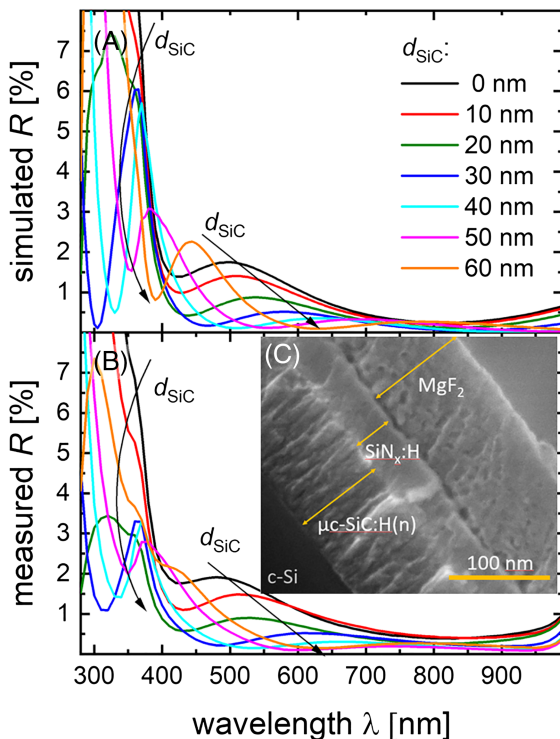

FIGURE 4 Reflectance of triple-layer ARC as presented in Figure 1 with (A) simulated using OPAL2 and also (B) measured on fabricated samples. (C) SEM image of triple-layer cross section for fine adjustment of layer thicknesses [Colour figure can be viewed at wileyonlinelibrary.com]
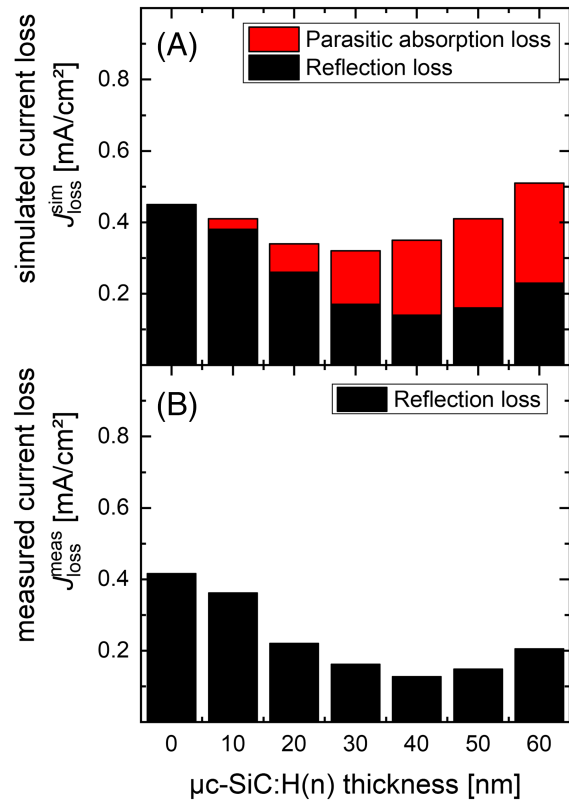
density loss ($J^{sim,R}$) decreases from 0.45 to 0.14 mA/cm^2 by increasing the d_{SiC} from 0 to 40 nm. For d_{SiC}, larger than 40 nm $J^{sim,R}$ increases. For the current density losses that were derived from reflectance spectra of the fabricated ARC samples ($J^{meas,R}$), we observe the same trend. The $J^{meas,R}$ decreases from 0.42 to 0.13 mA/cm^2 by increasing the d_{SiC} from 0 to 40 nm. The difference between $J^{sim,R}$ and $J^{meas,R}$ is within the error range. We further show the simulated parasitic absorption current density loss ($J^{sim,abs}$) in Figure 5 that was calculated from the extinction coefficient of μc-SiC:H(n). We observe that $J^{sim,abs}$ increases from 0 to 0.28 mA/cm^2 for d_{SiC} increasing from 0 to 60 nm. Summing reflection and absorption current densities, the lowest *simulated* total current density loss is 0.32 and 0.31 mA/cm^2 for the *measured* case, both at d_{SiC} of 30 nm.

For more sophisticated evaluation of the front side cell design, a state-of-the-art IBC-SHJ-solar cell was simulated using Sentaurus TCAD for the following front side concepts:

i. 108 nm MgF_2/75 nm SiN_x:H/30 nm μc-SiC:H(n),

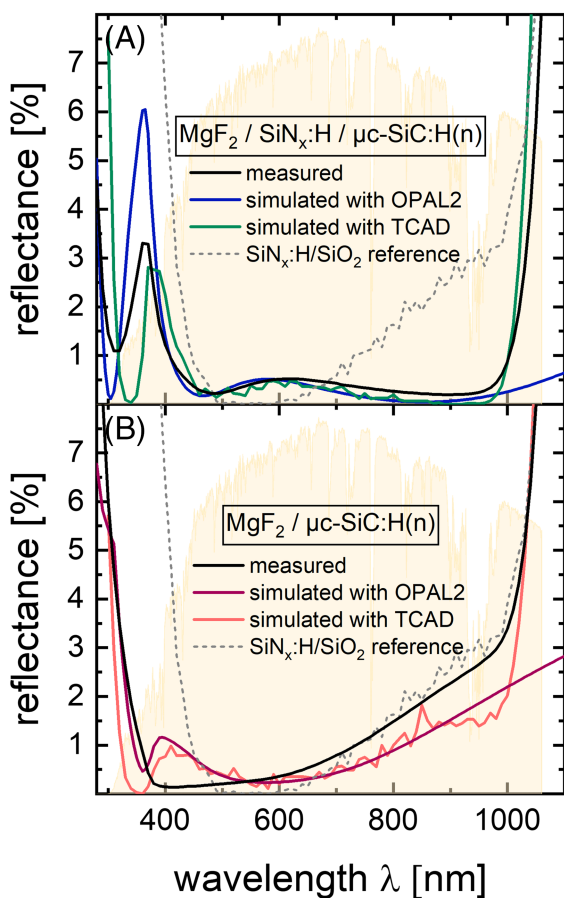**FIGURE 6** Comparison of reflectance of (A) 108 nm MgF$_2$/75 nm SiN$_x$:H/30 nm μc-SiC:H(n) and (B) 108 nm MgF$_2$/30 nm μc-SiC:H(n) antireflection coatings to state-of-the-art 60 nm SiN$_x$:H/10 nm SiO2 antireflection coating, where the reflectance was either measured on fabricated samples or calculated from OPAL2 and TCAD simulations. In background, the part of the AM1.5G sun spectrum is indicated, which should be transmitted through the front side layers to be absorbed by the c-Si [Colour figure can be viewed at wileyonlinelibrary.com]

ii. 108 nm MgF$_2$/30 nm μc-SiC:H(n),

iii. 60 nm SiN$_x$:H/10 nm SiO$_2$.

The resulting reflectance spectra are shown in Figure 6 together with measured reflectance spectra from fabricated samples and resulting spectra from OPAL2 simulations. For both cases, (i) and (ii), the simulated spectra from TCAD and OPAL2 are very similar and lead to reflectance <1% for the wavelength range of 500 to 800 nm. The measured and simulated spectra are congruent within the error range. In comparison, the simulated reflectance of the SiN$_x$:H/SiO$_2$ state-of-the-art reference (case iii) exhibits a strong maximum with >20% reflectance at ~400 nm, becomes zero for 500 to 600 nm, and increases again for wavelengths >600 nm. The derived values for the simulated total current density loss are (i) 0.47, (ii) 0.62, and (iii) 1.09 mA/cm^2, respectively. More details regarding corresponding reflection and parasitic absorption current density losses are listed in Table 1.

TABLE 1 Optical losses of ARC concepts simulated by Sentaurus TCAD

ARC Concepts	Front Parasitic Absorption Loss, mA/cm	Front Reflection Loss, mA/cm^2	Total Front Loss, mA/cm^2
108 nm MgF$_2$/75 nm SiN$_x$:H/30 nm μc-SiC:H(n)	0.15	0.32	**0.47**
108 nm MgF$_2$/30 nm μc-SiC:H(n)	0.15	0.47	**0.62**
60 nm SiN$_x$:H/10 nm SiO$_2$	0.21	0.88	**1.09**

Notes. Corresponding reflectance spectra are shown in Figure 6.

TABLE 2 Solar cell parameters for different ARC concepts calculated from Sentaurus TCAD simulation for low-cost c-Si wafer with a bulk lifetime of 12 milliseconds

	108 nm MgF$_2$/75 nm SiN$_x$:H/30 nm μc-SiC:H(n)	108 nm MgF$_2$/30 nm μc-SiC:H(n)	60 nm SiN$_x$:H/10 nm SiO$_2$
J_{sc}, mA/cm^2	42.18	42.24	41.84
V_{oc}, mV	738	738	738
FF, %	85.19	85.19	85.18
η, %	26.51	26.55	26.29

The resulting solar cell parameters of all three cases, which were obtained from Sentaurus TCAD simulation, are summarized in Table 2. For the simulations, a charge carrier lifetime in the c-Si bulk (τ_{bulk}) of 12 milliseconds was assumed, which corresponds to high-quality wafer. The main difference between the cases was found in J_{sc}, which is highest for (ii) the MgF$_2$/μc-SiC:H(n) stack (42.24 mA/cm^2), followed by (i) the MgF$_2$/SiN$_x$:H/μc-SiC:H(n) stack (42.18 mA/cm^2), and is lowest for (iii) the SiN$_x$:H/SiO$_2$ reference stack (41.84 mA/cm^2). For τ_{bulk} = 2 ms, which corresponds to cheap low-quality wafer, the solar cell parameters are smaller. For an IBC solar cell with (ii) the MgF$_2$/μc-SiC:H(n) ARC front side, this decreases the results in power conversion efficiency (η) to 25.2%, J_{sc} to 42.0 mA/cm^2, open-circuit voltage (V_{oc}) to 733 mV, and fill factor (FF) to 82.1%.

4 | DISCUSSION

Wide bandgap μc-SiC:H(n) used on top of a wet-chemically grown silicon tunnel oxide shows the ability to reach iV_{oc} > 740 mV and J_0 < 4 fA/cm^2. This impressive passivation was achieved on double-side textured, phosphorus-doped, Czochralski grown c-Si wafers with a resistivity of 1.0 Ωcm and a thickness of 170 μm. The iV_{oc} values are close to the best V_{oc} values reported so far for SHJ technology, where the best values are currently at 744 mV,[22,23] for wafers with

comparable thickness. For a wafer thickness of 165 μm, the estimated practical limit for iV_{oc} is 748 mV according to Yoshikawa et al.[23] To achieve such values close to the practical limit, Taguchi et al[22] claim that an ultraclean surface is needed, which was not assured for the sample preparation of this work as the HWCVD growth of μc-SiC:H(n) was not performed in a clean room. Compared with TOP-Con/POLO technology, the J_0 values of μc-SiC:H(n)/SiO$_2$ passivation are among the lowest J_0 values reported in the recent past for wet-chemically grown oxides ranging [13,24] from 1.5 to 20 fA/cm^2 [13,24-27]. The improvement in μc-SiC:H(n)/SiO$_2$ passivation as compared with our former work[7] was achieved by a convolution of an improved surface texture of the c-Si wafer, higher c-Si bulk lifetime, and optimized HWCVD process for the μc-SiC:H(n) deposition. It is important to notice that this excellent level of passivation only requires wet-chemical oxidation and HWCVD deposition of μc-SiC:H(n), which makes it a very simple and lean fabrication process. No further hydrogenation (through, eg, SiN$_x$, forming gas, Al$_2$O$_3$, and remote hydrogen plasma) and no further recrystallization at high temperatures are required. In order to understand the mechanisms for this lean passivation method, investigations are currently ongoing and will be the scope of another paper. The combination of solely wide bandgap materials gives rise to μc-SiC:H(n)/SiO$_2$ being a very transparent passivation.

To maximize J_{sc} of the final IBC solar cell, it was important to minimize the sum of reflection and parasitic absorption losses on the front side by tuning the thickness of μc-SiC:H(n). According to TCAD simulations, using 30 nm of μc-SiC:H(n) minimizes the total optical losses of the front side to 0.47 mA/cm^2 for MgF$_2$/SiN$_x$:H/μc-SiC:H(n) and to 0.62 mA/cm^2 for MgF$_2$/μc-SiC:H(n), which enable very high J_{sc}. For comparison, the total loss of the SiN$_x$:H/SiO$_2$ reference stack is 1.09 mA/cm^2.

Since extinction coefficients of MgF$_2$ and of SiN$_x$:H are zero over the whole wavelength range, all parasitic absorption of the developed ARC takes place in μc-SiC:H(n) layer, which absorbs significantly for λ < 520 nm. As compared with the parasitic absorption loss of 5 nm a-Si:H(i), which is approximately 1.5 mA/cm^2, 30 nm μc-SiC:H(n) absorbs 10 times less incoming sunlight (0.15 mA/cm^2), which shows the great potential of this layer. To further increase the transparency of the μc-SiC:H(n), a possible way is to increase the filament temperature during the HWCVD growth of μc-SiC:H(n) as it was reported before in previous studies.,[6,7] However, we also reported in Köhler et al[7] that higher filament temperatures decrease the μc-SiC:H(n)/SiO$_2$ passivation quality strongly. How to overcome this trade-off between transparency and passivation is currently under investigation. Additionally, the influence of the filament temperature on the refractive index needs to be studied, and possibly, the thicknesses of MgF$_2$ and μc-SiC:H(n) need to be readjusted. The even simpler case of MgF$_2$/SiO$_2$/c-Si, where MgF$_2$ would be evaporated on top of the SiO$_2$ tunnel oxide, is not taken into account since we found that the thin wet-chemical tunnel oxide alone cannot provide a decent passivation.

Finally, using MgF$_2$/μc-SiC:H(n) as ARC for IBC solar cells offers a simple and lean process flow and gives rise to the best simulated device performance of this work. It should be noticed that, although the total front losses are lowest using MgF$_2$/SiN$_x$:H/μc-SiC:H(n) ARC, the rear reflection losses are 2.11 mA/cm^2, whereas they are only 1.88 mA/cm^2 using MgF$_2$/μc-SiC:H(n) ARC. Consequently, the MgF$_2$/μc-SiC:H(n) ARC leads to slightly higher J_{sc} and η in the simulated devices. On low-cost wafer, it gives rise to an efficiency of 25.2% and a J_{sc} of 42.0 mA/cm^2. This is in the range of tunnel-junction IBC solar cells, which achieved a certified η of 25.0% and J_{sc} of 41.7 mA/cm^2 very recently[26,28] and which also follow the idea of simple fabrication process. On high-quality c-Si wafer, with τ_{bulk} = 12 ms, we calculated 26.6% for η, 42.24 mA/cm^2 for J_{sc}, 738 mV for V_{oc}, and 85.2% for FF. As compared, the best IBC solar cell fabricated by Kaneka gave rise to a certified η of 26.7%, 42.65 mA/cm^2 for J_{sc}, 738 mV for V_{oc}, and 84.9% for FF.[3] The main difference arises from 0.41 mA/cm^2 lower J_{sc} for the MgF$_2$/μc-SiC:H(n) stack, which might be increased by enhanced light trapping, further minimization of parasitic absorption in the μc-SiC:H(n) layer, and readjusting the thicknesses of MgF$_2$ and μc-SiC:H(n).

5 | CONCLUSION

In this study, the potential of a new passivation and antireflection layer stack for IBC solar cells was investigated. The passivation stack consists of a thin wet-chemically grown SiO$_2$ and HWCVD deposited wide bandgap μc-SiC:H(n) on top. Excellent passivation properties with a reproducible iV_{oc} of 742 mV and J_0 of 3.6 fA/cm^2 were achieved directly after the HWCVD deposition of μc-SiC:H(n), without any further treatments like recrystallization or hydrogenation. Because of its high transparency and its suitable refractive index, we developed MgF$_2$/μc-SiC:H(n) and MgF$_2$/SiN$_x$:H/μc-SiC:H(n) stacks as front side ARC for IBC solar cells. Both layer stacks showed very low reflectance that reduced the total optical losses of the front side in short-circuit current density to only 0.62 and 0.47 mA/cm^2, respectively. Finally, we simulated a solar cell with state-of-the-art IBC and with MgF$_2$/μc-SiC:H(n)/SiO$_2$/c-Si front side that lead to J_{sc} of 42.2 mA/cm^2, V_{oc} of 738 mV, FF of 85.2%, and a maximum power conversion efficiency of 26.6%.

ORCID

Manuel Pomaska https://orcid.org/0000-0002-9303-8395
Malte Köhler https://orcid.org/0000-0002-4869-4131
Paul Procel Moya https://orcid.org/0000-0003-4997-3551
Olindo Isabella https://orcid.org/0000-0001-7673-0163
Uwe Rau https://orcid.org/0000-0003-3526-3081

REFERENCES

1. Yoshikawa, K.,Kawasaki, H.Yoshida, W. et al. Silicon heterojunction solar cell with interdigitated back contacts for a photoconversion efficiency over 26%. *Nat. Energy*. Mar. 2017;2:17032.

2. Haase F, Hollemann C, Schäfer S, et al. Laser contact openings for local poly-Si-metal contacts enabling 26.1%-efficient POLO-IBC solar cells. *Sol. Energy Mater. Sol. Cells*. Nov. 2018;186:184-193.

3. Green MA, Dunlop ED, Levi DH, Hohl-Ebinger J, Yoshita M, Ho-Baillie AWY. Solar cell efficiency tables (version 54). *Prog. Photovolt. Res. Appl.* 2019;27(7):565-575.

4. Ingenito A, Nogay G, Jeangros Q, et al. A passivating contact for silicon solar cells formed during a single firing thermal annealing. *Nat. Energy*. Sep. 2018;3(9):800-808.

5. Holman ZC, Descoeudres A, Barraud L, et al. Current losses at the front of silicon heterojunction solar cells. *IEEE J. Photovolt.* Jan. 2012; 2(1):7-15.

6. Pomaska M, Richter A, Lentz F, et al. Wide gap microcrystalline silicon carbide emitter for amorphous silicon oxide passivated heterojunction solar cells. *Jpn. J. Appl. Phys.* Jan. 2017;56(2):022302.

7. Köhler M et al. Development of a transparent passivated contact as a front side contact for silicon heterojunction solar cells. *2018 IEEE 7th World Conference on Photovoltaic Energy Conversion (WCPEC) (A Joint Conference of 45th IEEE PVSC, 28th PVSEC 34th EU PVSEC)*. 2018; 3468-3472.

8. Chen T, Köhler F, Heidt A, Carius R, Finger F. Hot-wire chemical vapor deposition prepared aluminum doped p-type microcrystalline silicon carbide window layers for thin film silicon solar cells. *Jpn. J. Appl. Phys.* Jan. 2014;53(5S1):05FM04.

9. Chen T, Huang Y, Wang H, et al. Microcrystalline silicon carbide thin films grown by HWCVD at different filament temperatures and their application in n-i-p microcrystalline silicon solar cells. *Thin Solid Films*. Apr. 2009;517(12):3513-3515.

10. Miyajima S, Irikawa J, Yamada A, Konagai M. High-quality nanocrystalline cubic silicon carbide emitter for crystalline silicon heterojunction solar cells. *Appl. Phys. Lett.* Jul. 2010;97(2):023504.

11. Banerjee C, Narayanan KL, Haga K, et al. Fabrication of microcrystalline cubic silicon carbide/crystalline silicon heterojunction solar cell by hot wire chemical vapor deposition. *Jpn. J. Appl. Phys.* Jan. 2007; 46(1):1-6.

12. Köhler M, Pomaska M, Lentz F, Finger F, Rau U, Ding K. Wet-chemical preparation of silicon tunnel oxides for transparent passivated contacts in crystalline silicon solar cells. *ACS Appl. Mater. Interfaces*. May 2018;10(17):14259-14263.

13. Richter A, Benick J, Feldmann F, Fell A, Hermle M, Glunz SW. n-Type Si solar cells with passivating electron contact: identifying sources for efficiency limitations by wafer thickness and resistivity variation. *Sol. Energy Mater. Sol. Cells*. Dec. 2017;173:96-105.

14. Zhao J, Wang A, Green MA, Ferrazza F. 19.8% Efficient 'honeycomb' textured multicrystalline and 24.4% monocrystalline silicon solar cells. *Appl. Phys. Lett.* Oct. 1998;73(14):1991-1993.

15. Theiss W., "Hard- and Software for Optical Spectroscopy." [Online]. Available: www.mtheiss.com.

16. Baker-Finch SC, McIntosh KR. A freeware program for precise optical analysis of the front surface of a solar cell. *2010 35th IEEE Photovoltaic Specialists Conference (PVSC)*. 2010;002184-002187.

17. Procel P, Ingenito A, De Rose R, et al. Opto-electrical modelling and optimization study of a novel IBC c-Si solar cell. *Prog. Photovolt. Res. Appl.* 2017;25(6):452-469.

18. Synopsis, "Sentaurus Device User." 2013.

19. Procel P, Yang G, Isabella O, Zeman M. Theoretical evaluation of contact stack for high efficiency IBC-SHJ solar cells. *Sol. Energy Mater. Sol. Cells*. Nov. 2018;186:66-77.

20. Procel P, Yang G, Isabella O, Zeman M. Numerical simulations of IBC solar cells based on poly-Si carrier-selective passivating contacts. *IEEE J. Photovolt.* Mar. 2019;9(2):374-384.

21. Green MA. Self-consistent optical parameters of intrinsic silicon at 300 K including temperature coefficients. *Sol. Energy Mater. Sol. Cells*. Nov. 2008;92(11):1305-1310.

22. Taguchi M, Yano A, Tohoda S, et al. 24.7% Record efficiency HIT solar cell on thin silicon wafer. *IEEE J. Photovolt.*. Hercules Workshop, Jan. 2014;4(1):96-99.

23. Yoshikawa K., "Crystalline silicon heterojunction solar cell exceeding 26% conversion efficiency," *presented at the Hercules workshop*, Berlin, Oct-2016.

24. Peibst R., Römer U., Larionova Y., Rienäcker M., Merkle A., Folchert N., Reiter S., Turcu M., Min B., Krügener J., Tetzlaff D., Bugiel E., Wietler T., Brendel R., "Working principle of carrier selective poly-Si/c-Si junctions: is tunneling the whole story?," *Sol. Energy Mater. Sol. Cells*, vol. 158, Part 1, pp. 60–67, Dec. 2016.

25. Gan JY, Swanson RM. Polysilicon emitters for silicon concentrator solar cells. *IEEE Conference on Photovoltaic Specialists*. 1990;1: 245-250.

26. Glunz S. *et al.*, "The irresistible charm of a simple current flow pattern—approaching 25% with a solar cell featuring a full-area back contact," *Proc. 31h Eur. Photovolt. Sol. Energy Conf. Hambg. Ger. Sept. 14-18 2015*, 2015.

27. Yan D, Cuevas A, Bullock J, Wan Y, Samundsett C. Phosphorus-diffused polysilicon contacts for solar cells. *Sol. Energy Mater. Sol. Cells*. Nov. 2015;142:75-82.

28. Lachenal D, Papet P, Legradic B, et al. Optimization of tunnel-junction IBC solar cells based on a series resistance model. *Sol. Energy Mater. Sol. Cells*. Sep. 2019;200:110036.

SUPPORTING INFORMATION

Additional supporting information may be found online in the Supporting Information section at the end of this article.